On the Consistency of the Hydrodynamic and the Monte Carlo Models

B. Meinerzhagen, R. Thoma, H.J. Peifer, W.L. Engl
Institut für Theoretische Elektrotechnik
University of Aachen, Kopernikusstr. 16, 5100 Aachen, W-Germany
Phone: +49 241 80 3904, Fax: +49 241 874596

Abstract

The agreement which can be achieved between the hydrodynamic and the Monte Carlo model on the device level based on the consistency of both models under homogeneous conditions is briefly reviewed. The influence of heat flux and thermal diffusion on steady state velocity overshoot is examined within one-dimensional test structures.

1 Introduction

About a decade ago the Monte Carlo model (MCM) (solving Boltzmann's transport equation (BTE)) and the hydrodynamic model (HDM) (solving moment equations which can be derived from BTE under appropriate assumptions) started to be of increasing interest because hot carrier effects became more and more important for device design. At that time these models often were developed independently and sometimes they even seemed to play a competitive role. However in more recent years it turned out that the most beneficial role of the HDM for device design could be that of a bridge making the superior modeling accuracy of the MCM available for device design without significantly changing the user interface for the designers which are familiar with the handling and the computational speed of the drift diffusion model. For this bridging function consistency between the MCM and the HDM is of key interest. In the beginning is was unclear whether the HDM would be capable of replaying the MCM results with sufficient accuracy and even quite discouraging results were published [1] in this respect. Meanwhile at least for the steady state unipolar electron transport in Si MOSFETs it has been proven [2], [3] that a degree of consistency is achievable between both models which should be sufficient for most design applications today and in the near future. Many people have contributed to this development but instead of giving a broad overview over these contributions, in this paper we try to exemplify the achievable consistency within the framework of the generalized hydrodynamic model (GHDM) [2]. In the next chapter the results which have been achieved by adapting the GHDM to the MCM entirely under homogeneous conditions are briefly reviewed. In a subsequent section the modeling of steady state velocity overshoot with the GHDM is discussed.

2 GHDM adaptation to MC under homogeneous conditions

In [2] the GHDM is derived from BTE without assuming a parabolic band structure. Therefore the GHDM is better suited to incorporate nonparabolic band structure effects than previous HD models. On the other hand besides other assumptions (see [2]) it is still based on the relaxation time approximation. The steady state version of the GHDM for unipolar electron transport is given below:

$$
\begin{aligned}
\varepsilon\, \Delta\Psi &= -q\ (p - n + N_D - N_A) \\
\nabla \cdot J &= qR \\
J &= -\frac{q}{m^*}\left\{\tau_i^* qn\nabla\Psi - \tau_i kT^*\nabla n - f_{td}\,\tau_i n\nabla kT^*\right\} \\
\nabla \cdot S &= -J\cdot\nabla\Psi - \frac{3}{2}k\left\{n\tau_w^{*-1}(T^* - T_{eq}) + T^*R\right\} \\
S &= -\frac{5}{2q}kT^*\tau_s^*\tau_i^{*-1}\left\{J + f_{hf}\,\frac{q}{m^*}\tau_i n\nabla kT^*\right\}
\end{aligned}
$$

All symbols have their usual meaning and are defined in [2]. Moreover as in [2] $f_{hf} = f_{td} = 1$ is assumed throughout this section. Within the framework of the above GHDM impact ionization is described by the nonlocal electric field line based lucky electron model reported in [5].

Within the GHDM relaxation times $\tau_i^*, \tau_i, \tau_w^*, \tau_s^*$ are assumed to be functions of local electron temperature T^* and doping. Therefore as demonstrated in [2] and [3] relaxation times as well as the parameters for the lucky electron model (besides threshold energy for which an effective value of $1.75eV$ is adopted in agreement with [4]) can be extracted from a MCM under homogeneous material and field conditions. This is exemplified in figures 1 and 2 showing τ_i^* as a function of doping and electron temperature as well as the impact ionization coefficient α as a function of inverse electric field as they have been extracted from MC under homogeneous conditions. The model parameters of the relaxation time and impact ionization models within the GHDM are extracted from such curves such that parameter extraction on the device level is avoided.

The extraction procedure itself does not depend on the details of the MCM like scattering and band structure models and can be performed for different MCMs with comparable success with respect to the agreement of both models on the device level. However for the agreement of the GHDM with experimental data the quality of the underlying MCM is of course crucial. The MC multi-particle model used to generate the results shown in this paper is based on the high energy band structure model reported in [6] and the impact ionization model given in [7]. The impact ionization model has been derived consistent to the high energy band structure model.

The agreement of GHDM spatial distributions with the MC reference due to the extraction procedure outlined above is exemplified in figures 3 and 4. In these figures spatial distributions of electron density and impact ionization rate from both models are compared within the drain region of a typical n-channel LDD-MOSFET with $L_{eff} = 0.7\mu m$. In [3] it has been demonstrated that a comparable agreement of spatial distributions as well as drain and substrate currents can be achieved at least down to effective channel lengths of $0.3\mu m$ and down to a drain bias of $3V$ under peak substrate current condition.

3 Modeling of steady state velocity overshoot

Steady state velocity overshoot in silicon is very often monitored based on 1D $N^+ - N - N^+$ test structures [9], [10], [8]. The most common example (labeled example 1 in this paper) consists of three homogeneously doped regions with $N^+ = 5\cdot 10^{17}cm^{-3}$ and $N = 2\cdot 10^{15}cm^{-3}$), respectively. The lowly doped region is $0.4\mu m$ long and the length of the highly doped regions is $0.1\mu m$. The applied bias is usually 1.5V. It is well known for this example that the spatial velocity distributions resulting from many HD models show (spurious) velocity overshoot peaks within the N-region close to the junction with the N^+-region having the higher potential. Such peaks are never found in respective MC results. Moreover it is known that these peaks can be reduced and the agreement with MC improved by reducing the components of electron current density J and energy flux density S being related to the gradient of electron temperature namely the thermal diffusion current and the heat flux density, respectively. This has been shown for a scaled down [8] as well as for a vanishing [10] heat flux component. In [9] the same was shown for a vanishing thermal diffusion component.

Moreover in [11] it could be shown that already in the region of linear transport the assumption $f_{hf} = f_{td} = 1$ which is made within the GHDM mainly due to the relaxation time approximation is valid only for high doping levels, whereas for low doping f_{td} and f_{hf} are substantially lower than one.

In order to get more information concerning the appropriate size of f_{td}, f_{hf}, the GHDM has been modified to allow for values of f_{td}, f_{hf} different from 1. With this modified GHDM example 1 was simulated with different values for f_{td} and f_{hf}, respectively. Moreover in order to get a broader test base an additional example (example 2) was simulated. Example 2 has been derived from example 1 by increasing the doping by a factor of 100 and decreasing length by a factor of 4. The results of these simulations in comparison with the appropriate MC reference simulations are summarized in figures 5 to 10. Figure 5,6 and 9,10 show that without modifications ($f_{td} = f_{hf} = 1$) the spurious velocity overshoot is clearly observable within the results of the GHDM. Furthermore it can be concluded from figures 6 and 10 that even a vanishing thermal diffusion component without changing the heat flux density is not sufficient to completely remove the spurious velocity overshoot. This can be observed in [9] as well. In addition when changing f_{td} from 1 to 0 the terminal current deviation between the MCM and the GHDM is increased from 7% to 14% for example 1 and from 4% to 27% for example 2. Hence terminal current accuracy is getting worse though spurious velocity overshoot is decreased. Finally the agreement of the temperature distribution is getting worse as well with decreasing f_{td} since figure 8 shows that the location of the temperature maximum is shifted further away from the respective MC position. This happens not only for example 2 but can be observed for example 1 as well.

Decreasing heat flux while leaving thermal diffusion unchanged yields more encouraging results. In figures 5 and 9 it is demonstrated that the spurious velocity overshoot vanishes completely when heat flux is scaled down by a factor of 4 (example 1) or 8 (example 2), respectively. This is in good agreement with [8]. At the same time current accuracy improves from 7% to 6% for example 1 and from 4% to 2% for example 2. In addition the position of the temperature maximum is improved as well when heat flux is decreased (figure 7). Again this can be observed for example 1 as well.

4 Conclusion

It has been demonstrated that adapting the GHDM to the MCM under homogeneous conditions yields a good agreement between both models for MOSFETs down to effective channel lengths of $0.3\mu m$. Since this agreement is not significantly influenced if thermal diffusion or heat flux are decreased as discussed in section 3, both flux components can be modified in order to improve the modeling of steady state velocity overshoot while keeping previous results [2], [3] still valid in principle. In the framework of the GHDM it turns out at least for the case of $N^+ - N - N^+$ test structures that for a more accurate modeling of velocity overshoot only the heat flux term within the GHDM needs to be corrected. Hence only that term in the GHDM, which originates from a forth order moment of BTE and is therefore considered to be the least accurate anyway, has to be modified.

References

[1] M. Tomizawa, K. Yokoyama, A. Yoshii, IEEE Trans. on CAD, vol. CAD-7, p. 254, 1988

[2] R. Thoma, A. Emunds, B. Meinerzhagen, H.J. Peifer, W.L. Engl, IEEE Trans. on Electron Devices, vol. ED-38, pp. 1343, 1991

[3] H.J. Peifer, B. Meinerzhagen, R. Thoma, W.L. Engl, IEDM Tech. Dig., p. 131, 1991

[4] R. van Overstraaten, H. De Man, Solid State Electronics, p. 583, 1970

[5] B. Meinerzhagen, IEDM Tech. Dig., p. 504, 1988

[6] R. Brunetti, C. Jacoboni, F. Venturi, E. Sangiorgi, B. Ricco, Solid State Electronics, vol. 32, p. 1663, 1989

[7] R. Thoma, H.J. Peifer, W.L. Engl, W. Quade, R. Brunetti, C. Jacoboni, J. Appl. Phys., vol. 69(4), p.2300, 1990

[8] A. Gnudi, F. Odeh, M. Rudan, Europ. Trans. on Telecom. and rel. Technol., vol. 1, p. 307, 1990

[9] D. Chen, E.C. Kan, U. Ravaioli, C.-W. Shu, R.W. Dutton, IEEE Elec. Dev. Letters, vol. 13, p. 26, 1992

[10] T. Bordelon, X.-L. Wang, C.M. Maziar, A.F. Tasch, IEDM Tech Dig., p. 353, 1990

[11] R. Thoma, K.P. Westerholz, H.J. Peifer, W.L. Engl, Semicond. Sci. Technol., vol. 7, p. B328, 1992

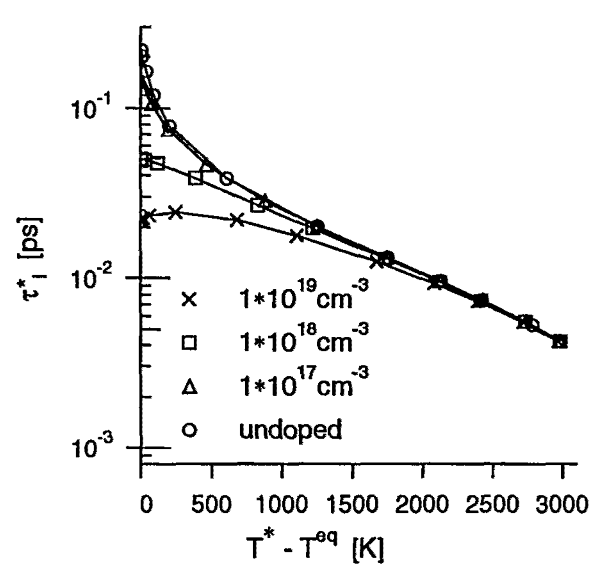

Figure 1: Momentum relaxation time τ_i^* extracted from the MCM under homogeneous conditions.

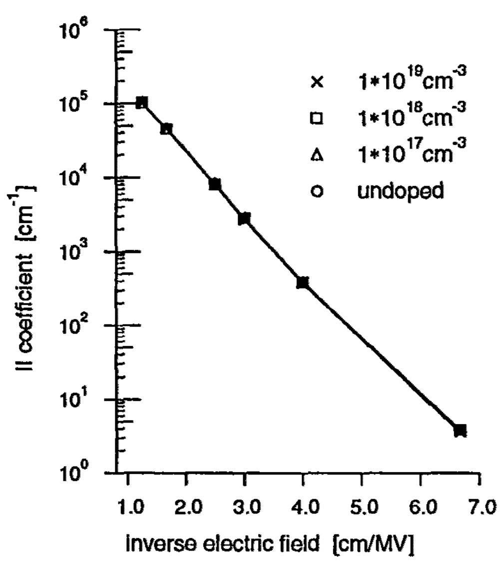

Figure 2: Impact ionisation coefficient α extracted from the MCM under homogeneous conditions.

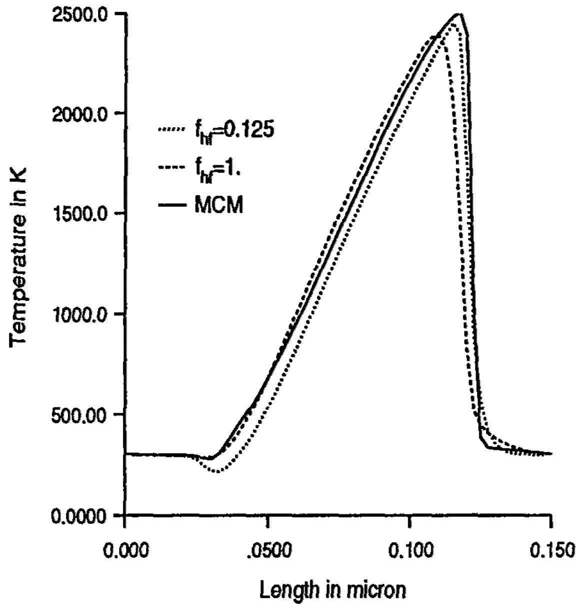

Figure 7: Comparison of spatial electron temperature distributions from the MCM and the modified GHDM for example 2 and different f_{hf} ($f_{td} = 1$).

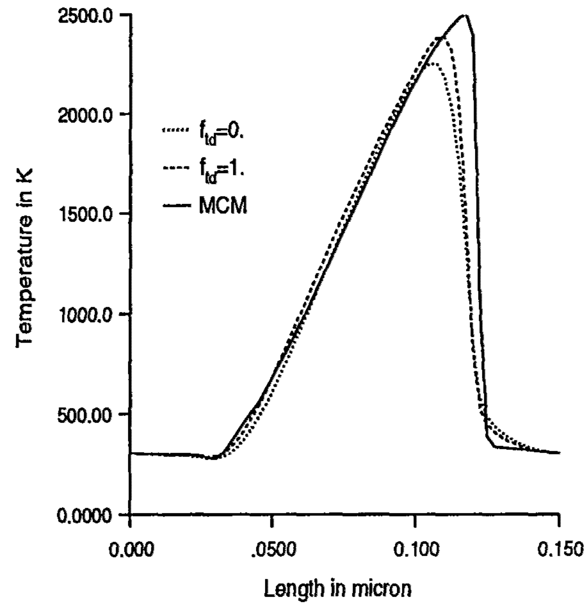

Figure 8: Comparison of spatial electron temperature distributions from the MCM and the modified GHDM for example 2 and different f_{td} ($f_{hf} = 1$).

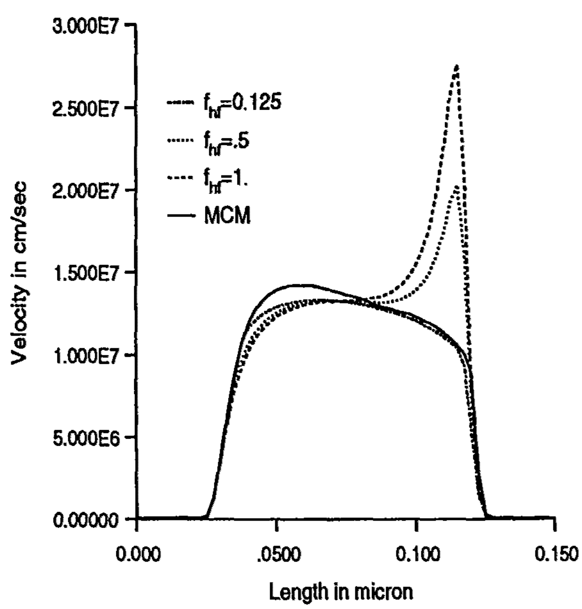

Figure 9: Comparison of spatial velocity distributions from the MCM and the modified GHDM for example 2 and different f_{hf} ($f_{td} = 1$).

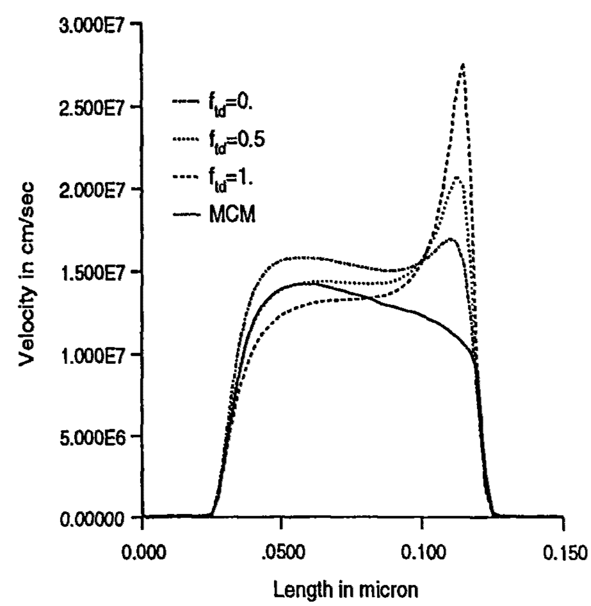

Figure 10: Comparison of spatial velocity distributions from the MCM and the modified GHDM for example 2 and different f_{td} ($f_{hf} = 1$).

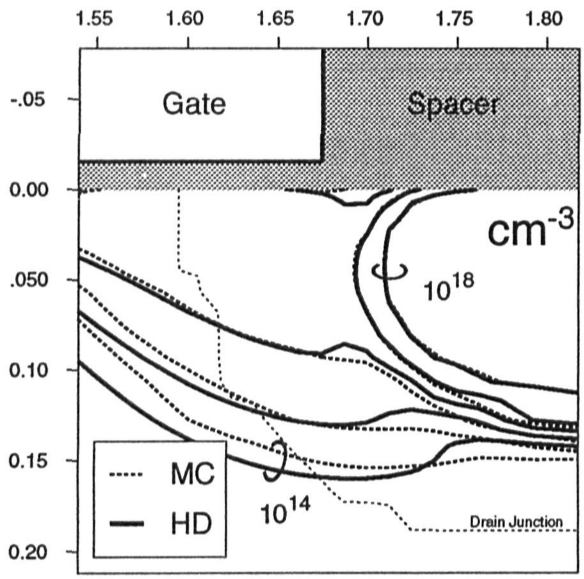

Figure 3: Comparison of spatial electron density distributions from the GHDM and the MCM within the drain region of a typical n-channel LDD-MOSFET ($L_{eff} = 0.7\mu m, V_D = 6V, V_G = 1.5V$).

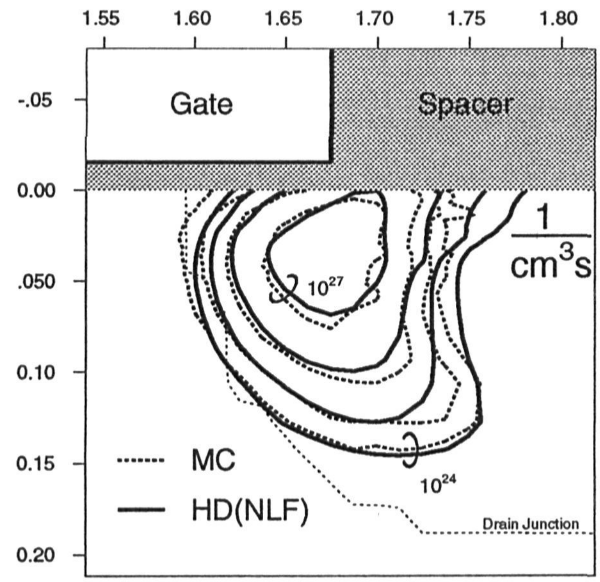

Figure 4: Comparison of spatial impact ionization rate distributions from the GHDM and the MCM within the drain region of a typical n-channel LDD-MOSFET ($L_{eff} = 0.7\mu m, V_D = 6V, V_G = 1.5V$).

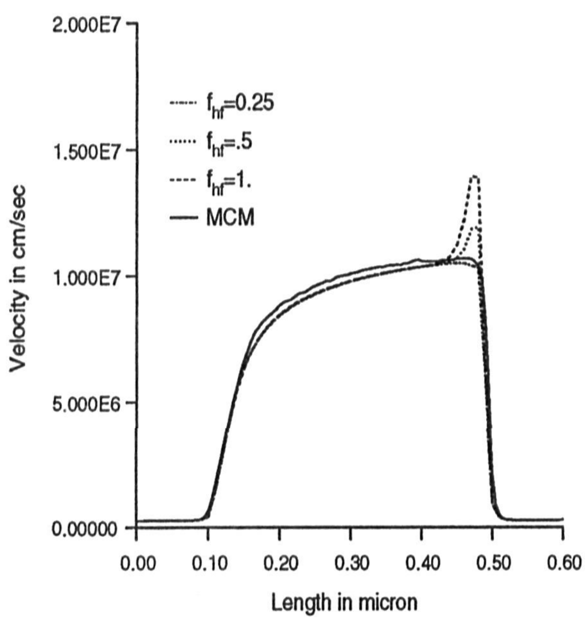

Figure 5: Comparison of spatial velocity distributions from the MCM and the modified GHDM for example 1 and different f_{hf} ($f_{td} = 1$).

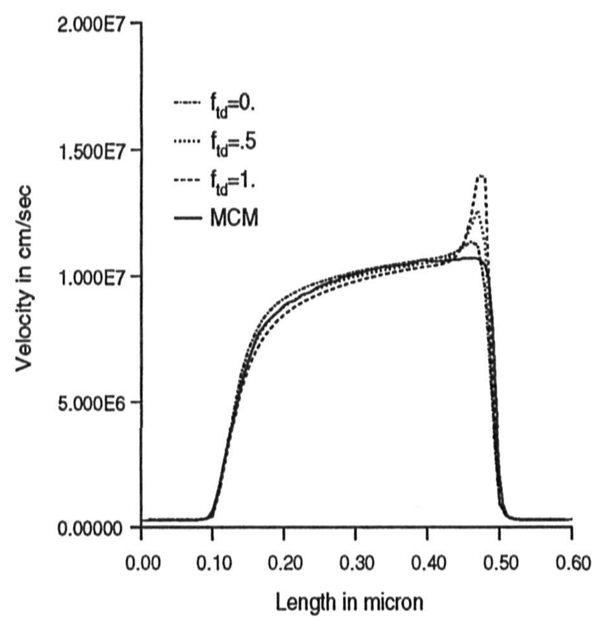

Figure 6: Comparison of spatial velocity distributions from the MCM and the modified GHDM for example 1 and different f_{td} ($f_{hf} = 1$).